

## Article

# Piezoelectric and Dielectric Properties in $\text{Bi}_{0.5}(\text{Na},\text{K})_{0.5}\text{TiO}_3\text{-xAg}_2\text{O}$ Lead-Free Piezoceramics

Xiaoming Chen <sup>1,2,\*</sup>  and Yunwen Liao <sup>2</sup><sup>1</sup> School of Materials and Energy Engineering, Guizhou Institute of Technology, Guiyang 550003, China<sup>2</sup> College of Chemistry and Engineering, China West Normal University, Nanchong 637009, China

\* Correspondence: chen-xm123@163.com

**Abstract:** Lead-free piezoceramics of  $\text{Bi}_{0.5}(\text{Na}_{0.825}\text{K}_{0.175})_{0.5}\text{TiO}_3$  with varying concentrations of  $x$  mol%  $\text{Ag}_2\text{O}$  ( $x = 0, 0.1, 0.3, 0.5, 0.7, 0.9$ , denoted as BNKT- $x$ A) were fabricated using the solid-state technique. An extensive investigation was undertaken to analyze the structural, piezoelectric, and dielectric properties of these piezoceramics in the presence of Ag ions. There is no evidence of any secondary solid solution in the BNKT- $x$ A piezoceramics. The ceramics with  $x$  mol%  $\text{Ag}_2\text{O}$  in BNKT still demonstrate the presence of both rhombohedral (R) and tetragonal (T) phases. The addition of  $\text{Ag}^+$  is helpful to increase the relative density of the BNKT- $x$ A piezoceramics. It is noteworthy that the BNKT-0.3 mol% A piezoceramics show remarkable improvements in their properties ( $d_{33} = 147$  pC/N,  $k_p = 29.6\%$ ,  $\epsilon = 1199$ ,  $\tan\delta = 0.063$ ). These improvements may be ascribed to the denser microstructure and the preservation of morphotropic phase boundaries between R and T phases caused by the appropriate addition of Ag cations. The addition of  $\text{Ag}^+$  results in the relaxor behavior of the BNKT- $x$ A ceramics, characterized by disorder among A-site cations. With the increase in temperature, the  $d_{33}$  value of BNKT- $x$ A ceramics does not vary significantly in the range of 25 to 125 °C, ranging from 127 to 147 pC/N (with a change of  $d_{33} \leq 13.6\%$ ). This finding shows that piezoelectric ceramics have a reliable performance over a certain operating temperature range.

**Keywords:** lead-free; ceramics; phase transition; relaxor behavior**Citation:** Chen, X.; Liao, Y.Piezoelectric and Dielectric Properties in  $\text{Bi}_{0.5}(\text{Na},\text{K})_{0.5}\text{TiO}_3\text{-xAg}_2\text{O}$  Lead-Free Piezoceramics. *Materials* **2023**, *16*, 5342. <https://doi.org/10.3390/ma16155342>

Academic Editors: Jörg Wallaschek, Mickaël Lallart, Guylaine Poulin-Vittrant and Hélène Debeda

Received: 30 June 2023

Revised: 26 July 2023

Accepted: 27 July 2023

Published: 29 July 2023



**Copyright:** © 2023 by the authors. Licensee MDPI, Basel, Switzerland. This article is an open access article distributed under the terms and conditions of the Creative Commons Attribution (CC BY) license (<https://creativecommons.org/licenses/by/4.0/>).

## 1. Introduction

Piezoceramics are extensively employed in various applications, including transducers, sensors, actuators, etc. However, it is worth noting that the majority of piezoelectric ceramics used are Pb-based, specifically  $\text{Pb}(\text{Zr}_{1-x}\text{Ti}_x)\text{O}_3$  (PZT). The presence of Pb in these ceramics raises concerns regarding environmental toxicity, particularly attributed to the volatilization of  $\text{PbO}$  in the sintering procedure. Consequently, it has resulted in the implementation of legislation in different countries, such as regulations on WEEE and restrictions on RoHS [1,2]. Hence, it is important to focus on the development of lead-free piezoceramics from an environmental perspective.

Lead-free piezoceramics should be classified into four main species:  $\text{BaTiO}_3$ -based [3,4],  $\text{Bi}_{0.5}\text{Na}_{0.5}\text{TiO}_3$ -based, Bi-layered [5], and niobate-based ceramics [6]. Among these,  $\text{Na}_{0.5}\text{Bi}_{0.5}\text{TiO}_3$  (BNT) lead-free ceramics were first synthesized by Smolenkii et al. in 1960 and exhibit a rhombohedral crystal phase around room temperature, with a  $T_c$  of 320 °C [7]. BNT ceramics display strong ferroelectricity, excellent piezoelectric performance, outstanding acoustic properties, and a lower sintering temperature compared to other systems [8,9]. As a result, BNT has become one of the most extensively studied Pb-free ceramics. However, pure BNT ceramics face challenges in practical applications due to their high coercive field and poor compactness. Currently, research on BNT-based ceramics primarily focuses on enhancing their performance through replacement and doping strategies. For instance, studies have been conducted on BNT- $\text{BaTiO}_3$  [10,11],  $\text{Bi}_{0.5}(\text{Na}_{1-x-y}\text{Li}_y\text{K}_x)_{0.5}\text{TiO}_3$  [12],  $\text{Bi}_{0.5}\text{Na}_{0.5}\text{TiO}_3\text{-K}_{0.5}\text{Bi}_{0.5}\text{TiO}_3$  (BNKT) [13],  $\text{Bi}_{0.5}\text{Na}_{0.5}\text{TiO}_3\text{-KNbO}_3$  [14],  $\text{Bi}_{0.5}\text{Na}_{0.5}\text{TiO}_3\text{-BaTiO}_3\text{-KNbO}_3$  [15],  $[(\text{K}_{0.175}\text{Na}_{0.825})_{0.5}\text{Bi}_{0.5}]_{1+x}\text{TiO}_3$  [16],

( $\text{Na}_{1/2}\text{Bi}_{1/2}\text{TiO}_3\text{-BaTiO}_3\text{-(Na}_{1/2}\text{K}_{1/2})\text{NbO}_3$  [17], and  $0.76\text{Bi}_{0.5}\text{Na}_{0.5}\text{TiO}_3\text{-Bi(Ni}_{2/3}\text{Nb}_{1/3})\text{O}_3\text{-0.24SrTiO}_3$  [18]. Among these materials, BNKT ceramics, particularly those near the morphotropic phase boundary (MPB) between the rhombohedral and tetragonal phases with  $0.16 \leq x \leq 0.2$ , exhibit excellent electrical properties, such as high ratios of  $k_t$  (the piezoelectric coupling coefficient) to  $k_p$  (the planar coupling coefficient). Furthermore, the incorporation of  $\text{Bi}_{0.5}\text{K}_{0.5}\text{TiO}_3$  into BNT can reduce the coercive field ( $E_c$ ) to a minimum of 4 kV/mm [13]. Nevertheless, the high sintering temperature required for this material can lead to the evaporation of Na and K [19].

Grinberg and Rappe [20] reported that the presence of Ag in perovskite solid solutions leads to significant polarization and piezoelectric responses due to the large distortion of Ag on the A-site, as observed in the  $\text{AgNbO}_3$  system [21]. Wu et al. discovered that when  $\text{Bi}_{0.5}\text{Ag}_{0.5}\text{TiO}_3$  is introduced into BNT-BT, the piezoceramics are still located at the R-T phase transformation. Additionally, these ceramics not only achieve dense structure but also have optimum electric performance ( $d_{33} = 172$  pC/N,  $k_p = 32.6\%$ ,  $k_t = 52.6\%$ ) [22]. Lin et al. observed a morphotropic phase boundary (MPB) in  $(\text{Li}_{0.075}\text{Na}_{0.925-x-y}\text{Ag}_y\text{K}_x)_{0.5}\text{Bi}_{0.5}\text{TiO}_3$  systems where  $\text{K}^+$ ,  $\text{Li}^+$  and  $\text{Ag}^+$  occupy part of the BNT lattices. Specifically, in the system with  $0.15 < x < 0.25$ , the presence of the morphotropic phase boundary, combined with a low coercive field, significantly enhances piezoelectric properties ( $d_{33} = 178\text{--}219$  pC/N,  $k_p = 35\text{--}39\%$ ,  $k_t = 44\text{--}51\%$ ) [23]. Liao et al. found that the substitution of  $\text{Ag}^+$  and  $\text{K}^+$  for Na ions in BNT results in the high performance of  $(\text{Na}_{1-x-y}\text{Ag}_y\text{K}_x)_{0.5}\text{Bi}_{0.5}\text{TiO}_3$  piezoceramics ( $d_{33} = 180$  pC/N,  $k_p = 0.35$ ) [24]. These studies suggest that the combination of the presence of Ag and phase boundary effects holds significant potential for the manufacture of BNKT-based ceramics with improved performance.

In this case, an appropriate amount of  $\text{Ag}_2\text{O}$  was introduced into BNT- $\text{Bi}_{0.5}\text{K}_{0.5}\text{TiO}_3$  to enhance its sinterability and performance. The traditional ceramic process is employed to prepare the piezoceramics. The structure and electrical properties are systematically studied. A comprehensive elucidation of the underlying mechanism is presented in detail.

## 2. Materials and Methods

According to the traditional ceramic preparation process,  $\text{Bi}_2\text{O}_3$  (Chenguang Chemical Co., Ltd., Qishan, China, AR, 99%),  $\text{TiO}_2$  (Zhongxing Electronic Materials Co., Ltd., Xiantao, China, AR, 99.5%),  $\text{Na}_2\text{CO}_3$  (Xilong Chemical Co., Ltd., Shantou, China, AR, 99.7%),  $\text{K}_2\text{CO}_3$  (Xilong Chemical Co., Ltd., Shantou, China, AR, 99.8%), and  $\text{Ag}_2\text{O}$  (Chenguang Chemical Co., Ltd., Qishan, China, AR, 99%) were used as starting materials. Based on the stoichiometric ratio of components, the system  $\text{Bi}_{0.5}(\text{Na}_{0.825}\text{K}_{0.175})_{0.5}\text{TiO}_3+x$  mol%  $\text{Ag}_2\text{O}$  ( $x = 0, 0.1, 0.3, 0.5, 0.7, 0.9$ , abbreviated as BNKT-xA) was weighed. The raw material was ball milled for 6~7 h, fully mixed and crushed, and presynthesized at 850~900 °C for 2 h. The synthesized ceramic powders were fully ground and added with the proper amount of binder PVA, and then granulated to obtain particles with good fluidity. The green sheets with thickness of 1.2~1.5 mm and diameter of 10 mm were obtained by dry pressing under a certain pressure, and then sintered at 1150~1200 °C for 2 h to obtain ceramics. Under the silicone oil at 80 °C, the piezoceramics were poled by a DC electric field of 4~5 kV/mm for 20~30 min, and then the electrical properties of the samples were measured after one day and night.

The phase structure of the piezoceramics was identified by XRD (Rigaku Dmax/RB, Tokyo, Japan). The surface of the piezoceramics was obtained by SEM (JSM-6510, JEOL, Akishima, Japan). The density of the ceramics was determined using the Archimedes method. The  $d_{33}$  of poled ceramic samples was measured by a Burlincourt-type  $d_{33}$  meter (ZJ-3A, Institute of Acoustic Academia Sinica, Beijing, China). The temperature-dependent dielectric properties were measured using an impedance analyzer (Agilent4284A, Santa Clara, CA, USA) and a custom-designed furnace. The measurements were conducted in the range of 25~500 °C with a heating rate of 2 °C/min. The  $k_p$  was determined using Onoe's formula, which involved analyzing the frequencies obtained from antiresonance and resonance measurements [25].

### 3. Results and Discussion

#### 3.1. Structure

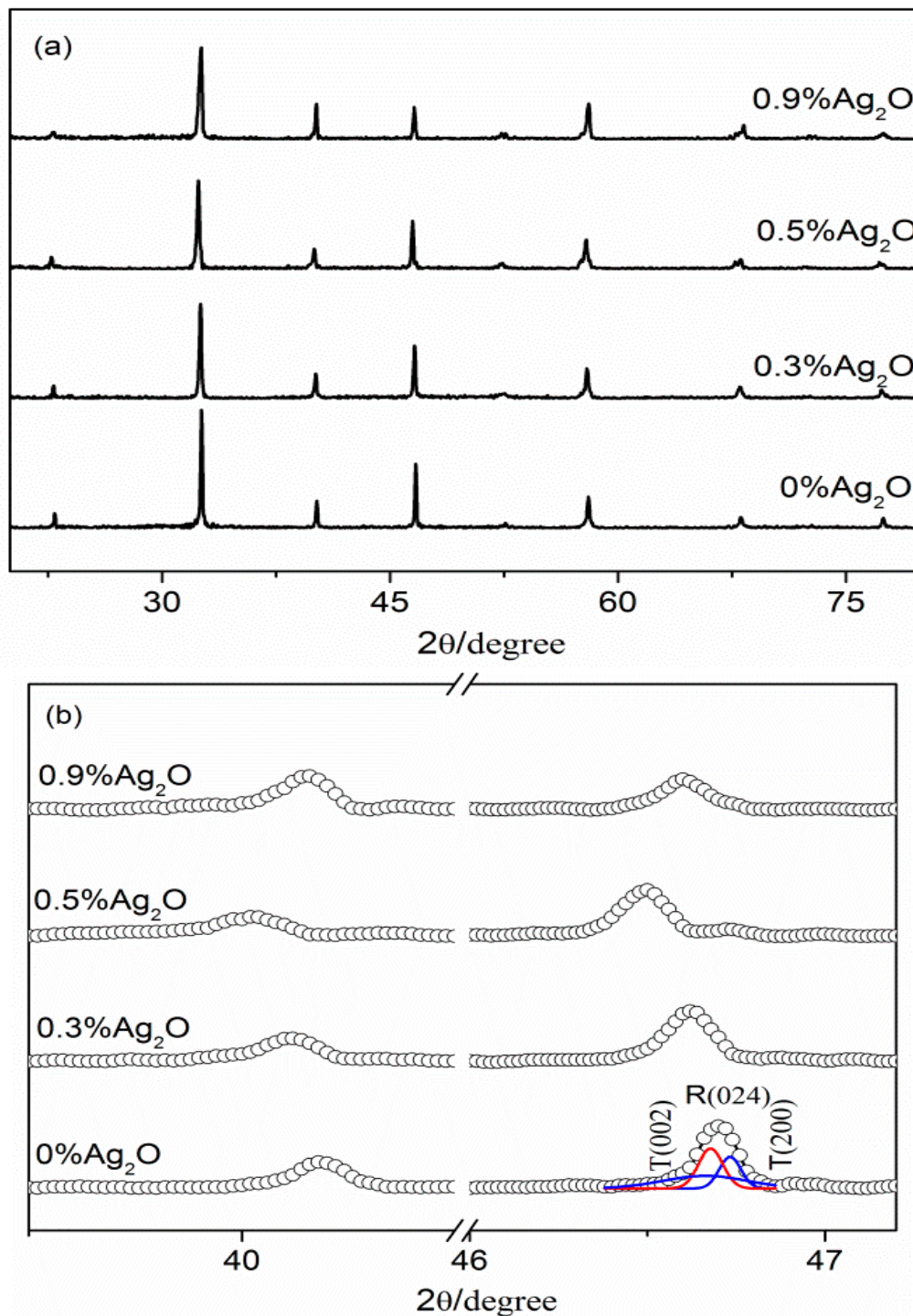
The XRD patterns of the BNKT-xA piezoceramics are presented in Figure 1. In Figure 1a, it is evident that all the structures of the BNKT-xA ceramics ( $x = 0\text{--}0.9\%$ ) show a single  $\text{ABO}_3$ -typed perovskite, indicating the substitution of Ag ions for A-site cations in the  $\text{Bi}_{0.5}(\text{K}, \text{Na})_{0.5}\text{TiO}_3$  lattices to form a homologous compound. The BNT-BKT piezoceramics are known to have a MPB ( $x = 0.16\text{--}0.20$ ) between the R and T phases. In order to investigate the crystal structure of the BNKT-xA piezoceramics, magnified XRD patterns within the  $2\theta$  range of  $39\text{--}47^\circ$  are given in Figure 1b. In Figure 1b, the miller index is used to check special peaks because of the R-T phase boundary. The peaks at  $46^\circ$  correspond to the rhombohedral (024) and tetragonal (002) phases, based on the  $R3c$  and  $P4bm$  space group (COD ID: 2103295; COD ID: 2102068) [26,27]. Hence, the observed peak splitting demonstrates that all the BNKT-xA piezoceramics are situated in the R-T MPB. Previous studies by Wu et al. demonstrated that for  $0 \leq y \leq 0.075$ , there is no significant change in the phase structure of  $(0.94-y)\text{Na}_{0.5}\text{Bi}_{0.5}\text{TiO}_3$ - $y\text{Bi}_{0.5}\text{Ag}_{0.5}\text{TiO}_3$ - $0.06\text{BaTiO}_3$  piezoceramics within the MPB range [22]. Similarly, Lin et al. observed that  $\text{Ag}^+$  substitution for A-site cations does not affect the phase transformation in  $\text{Bi}_{0.5}(\text{Na}_{0.75-y}\text{Li}_{0.075}\text{K}_{0.175}\text{Ag}_y)_{0.5}\text{TiO}_3$  piezoceramics ( $0.015 \leq y \leq 0.15$ ), which falls within the MPB [23]. Additionally, Liao et al. found that lower Ag content has no influence on the R-T phase transition in the  $(\text{K}_{0.175}\text{Na}_{0.825-y}\text{Ag}_y)_{0.5}\text{Bi}_{0.5}\text{TiO}_3$  system ( $y = 0.015\text{--}0.075$ ) [24]. Consistent with these previous reports, our results show a similar trend. Furthermore, with the appropriate addition of  $\text{Ag}^+$ , the diffraction peaks gradually shift to smaller angles. During the sintering process, the evaporation of A-site cations often results in the generation of oxygen vacancies in BNKT ceramics. However, the dopant of Ag ions effectively counteracts the loss of A-site cations, thereby reducing the occurrence of oxygen vacancies. It is well established that an abundance of oxygen vacancies can cause the contraction of unit cells and a movement of diffraction peaks towards higher angles [28–31]. Consequently, the observed decrease in the displacement of the (002) peaks at low angles in the BNKT-xA ceramics demonstrates a reduction in the presence of oxygen vacancies.

Figure 2 illustrates the surface morphology of BNKT-xA piezoceramics using SEM. It is evident that the ceramics exhibit distinct grain boundaries and a regular square shape. With the increase in  $\text{Ag}^+$  content, the tetragonal feature of the grains is further strengthened, resulting in a more uniform and homogeneous shape. Therefore, the appropriate addition of  $\text{Ag}^+$  ions contributes to the homogeneity of the ceramic grains. This finding is consistent with a previous study on  $\text{Bi}_{0.5}(\text{Na}_{0.825-y}\text{K}_{0.175}\text{Ag}_y)_{0.5}\text{TiO}_3$  ceramics [24]. Furthermore, the relative density of the piezoceramics goes up after the addition of  $\text{Ag}^+$ . All BNKT-xA ceramics have high densities ranging from  $5.62\text{--}5.71 \text{ g/cm}^3$ , which exceeds 95% of the theoretical values of  $\text{Bi}_{0.5}(\text{K}_{0.2}\text{Na}_{0.8})_{0.5}\text{TiO}_3$  ( $5.889 \text{ g/cm}^3$ ), as seen in Figure 3 [32]. The appropriate doping of  $\text{Ag}^+$  has enhanced the sinterability and densification of the BNKT-xA piezoceramics. This observation is likely due to the reduction in the evaporation of Na and K cations caused by the proper addition of  $\text{Ag}^+$ . The homogeneous structure and dense microstructure are particularly advantageous for enhancing the electric properties of BNKT-xA piezoceramics.

#### 3.2. Electrical Properties

Figure 4 illustrates the piezoelectric and dielectric properties of BNKT-xA piezoceramics. As the amount of  $\text{Ag}^+$  increases, both  $d_{33}$  and  $k_p$  gradually go up as well. When  $x = 0.3\%$ ,  $d_{33}$  gets to its peak value at  $147 \text{ pC/N}$ , the electromechanical coupling coefficient  $k_p$  peaks at 0.31 for  $x = 0.5\%$ . The incorporation of  $\text{Ag}^+$  enhances the piezoelectric properties of BNKT-xA ceramics compared to pure BNKT ceramics. This enhancement can be attributed to a mechanism in which the sintering process leads to the partial volatilization of sodium and potassium, creating vacancies. Ag ions occupy these vacancies within the crystal lattice, causing distortion in the perovskite structure. This distortion is helpful to the migration of domain walls, promoting the reversal of electric domains [33]. Additionally, the introduction of an appropriate amount of Ag ions results in denser ceramics, as depicted in Figures 2 and 3. The increased density allows for

sufficient polarization, thereby further improving the piezoelectric properties of the BNKT-xA ceramics. Furthermore, Figure 4b demonstrates that similar to the correlation between  $x$  and  $d_{33}$ , the relative permittivity attains its peak value (1199) at  $x = 0.3\%$ , subsequently diminishing as the concentration of  $\text{Ag}^+$  increases. The dielectric loss obtains its minimum value of 0.063 at  $x = 0.3\%$  before gradually increasing.



**Figure 1.** (a) XRD patterns of BNKT-xA piezoceramics; (b) the expanded XRD patterns of BNKT-xA piezoceramics in the range of 35–47°.

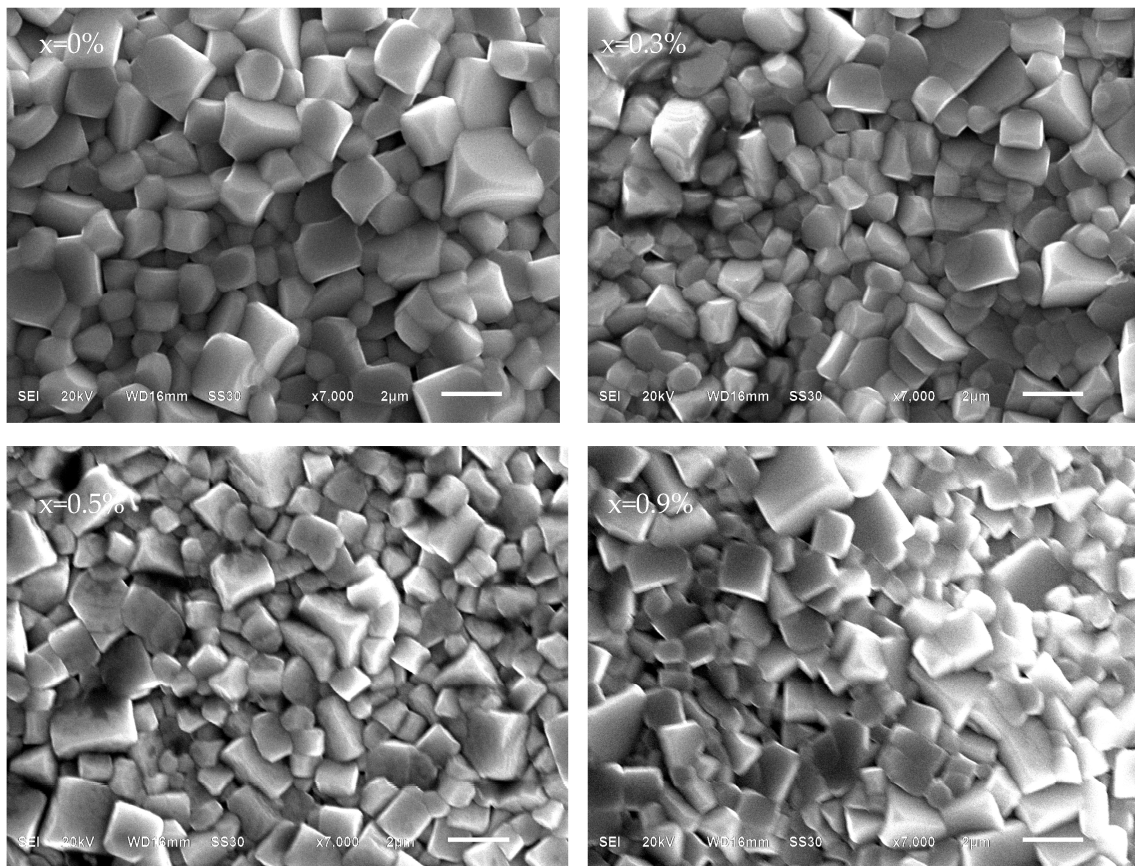


Figure 2. SEM surface micrographs of BNKT-xA ceramics.

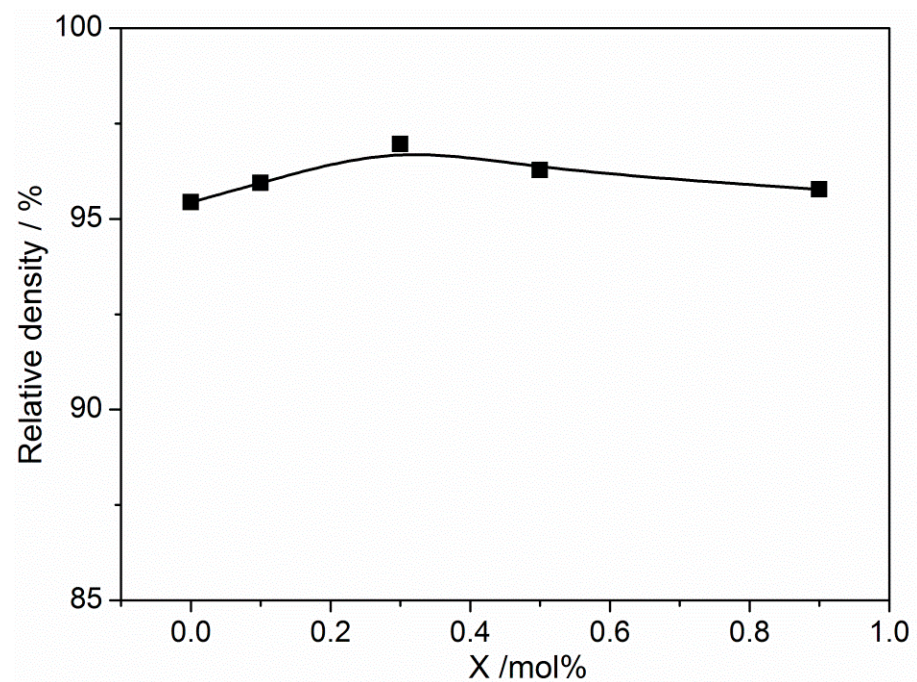
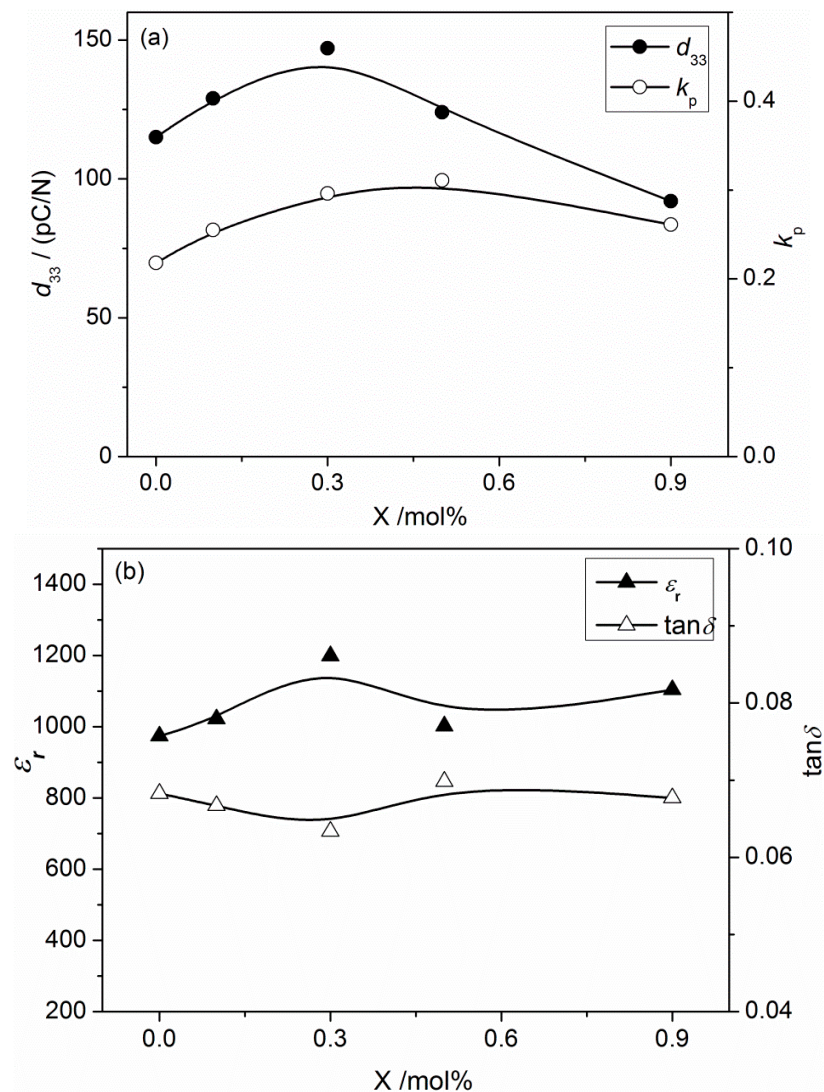


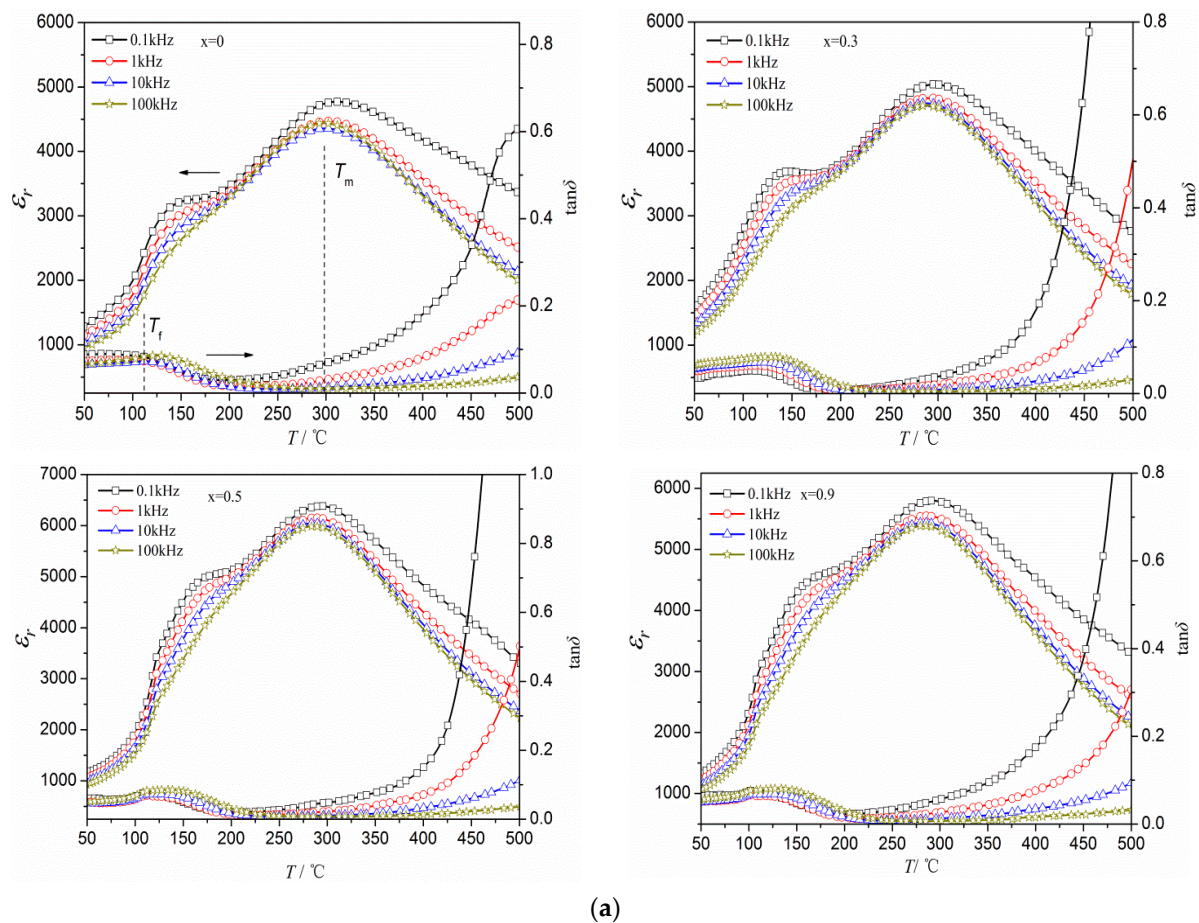
Figure 3. Relative density of BNKT-xA ceramics.



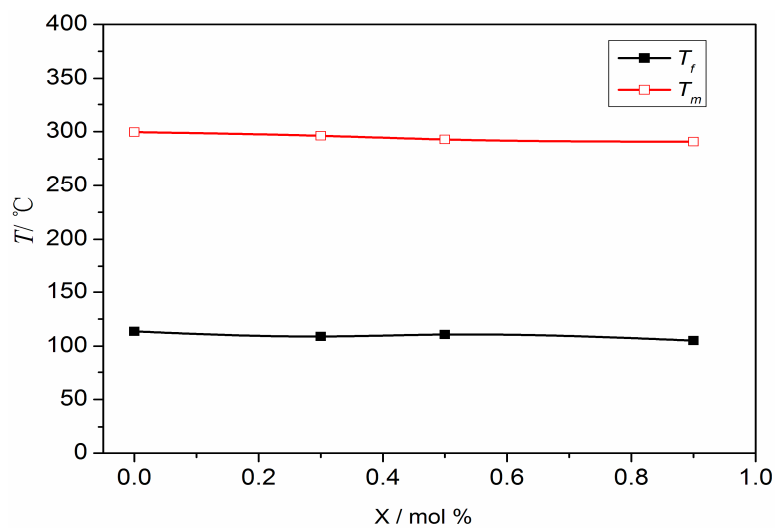
**Figure 4.** (a) Piezoelectric and (b) dielectric properties of BNKT-xA ceramics measured at 1 kHz.

### 3.3. Dielectric Properties

Figure 5a illustrates the variations of  $\epsilon_r$  and  $\tan\delta$  in BNKT-xA piezoceramics with respect to temperature and frequency. Similar to BNT-based piezoceramics, there are two phase transitions observed within the measured temperature range: a transition from a ferroelectric to an anti-ferroelectric phase transformation (at  $T_f$ ), and a transition from an anti-ferroelectric to a paraelectric phase transformation (at  $T_m$ ) [19,34,35]. A single peak at  $T_f$  is observed in the  $\tan\delta$ - $T$  curves of the ceramics, and  $\tan\delta$  goes up significantly at temperatures higher than  $T_m$  due to substantial leakage conduction [36,37]. The variations of  $\epsilon_r$  reveal that the temperature-dependent behavior of the piezoceramics reveals an increase in  $\epsilon_r$  as the temperature rises. This is characterized by a broadened peak around  $T_f$  and the attainment of the maximum value at  $T_m$ . In addition, with the addition of  $\text{Ag}^+$ , a slight decrease in  $T_f$  and  $T_m$  is observed among the different samples, as shown in Figure 5b.  $T_m$  serves as an indicator of the equilibrium of the oxygen octahedron, and it is able to be affected by the presence of ions [38]. Previous studies have demonstrated that the Ag-O bond has an energy of 221 kJ/mol, which is comparatively lower than the energy of K-O and Na-O bonds (271.5 kJ/mol, 270 kJ/mol) [39,40]. Hence, by properly adding  $\text{Ag}^+$ , Ag ions occupy the A-site in the  $\text{ABO}_3$ -typed lattice after the partial evaporation of alkali metal ions, thereby increasing the instability of oxygen octahedron and reducing  $T_m$  [39,41].



(a)



(b)

**Figure 5.** (a) Temperature dependence of dielectric properties for BNKT-xA piezoceramics. (b)  $T_f$  and  $T_m$  for BNKT-xA piezoceramics measured at 1 kHz.

In addition, the  $\epsilon_r$ - $T$  curves show prominent characteristics of the diffuse phase transition. Specifically, with an increase in frequency, the  $\epsilon_r$  exhibits a corresponding decrease, resembling the behavior of relaxor-like ferroelectric materials such as BNT-BT [10] and BNT-BKT [34]. Based on the aforementioned findings, it is evident that the temperature-dependent variation in the relative permittivity of BNKT-xA ceramics does not conform to the classical Curie-Weiss law when the temperature exceeds  $T_m$ . In order to describe the

diffusion of the phase transformation in the ferroelectric materials, a modified Curie–Weiss law is employed in our study [42].

The equation is as follows:

$$\frac{1}{\varepsilon_r} - \frac{1}{\varepsilon_{r,m}} = C(T - T_m)^\alpha \quad (1)$$

Here,  $\varepsilon_r$  and  $\varepsilon_{r,m}$  represent the dielectric constants at temperature  $T$  and  $T_m$ , respectively. The diffusion constant ( $\gamma$ ) is assumed to range between 1 and 2. If  $\gamma$  equals 1 or 2, the materials are referred to as normal or “complete” diffuse ferroelectrics. In contrast, when  $\gamma$  values fall within the range of 1 to 2, the materials are classified as relaxor ferroelectrics. Figure 6 illustrates the diffusion for BNKT- $x$ A piezoceramics at 1 kHz. Through linear regression analysis of the experimental data, the slope of fitting curves is determined to identify the value of  $\gamma$ . In this case, the value of  $\gamma$  ranges between 1.90 and 1.96, demonstrating that the BNKT- $x$ A piezoceramics exhibit a more diffuse behavior as the concentration of  $\text{Ag}^+$  increases. It can be reasonably ascribed to disorder among A-site cations caused by the presence of  $\text{Ag}^+$ . Based on Shannon’s ionic radius, the radius of  $\text{Ag}^+$  is 1.26 Å. It is similar to that of  $\text{K}^+$  (1.33 Å) and  $\text{Na}^+$  (0.98 Å) [29]. Thus,  $\text{Ag}^+$  can occupy the A-site vacancies in the  $\text{ABO}_3$ -typed structure after part of Na and K evaporates during the sintering procedure. Consequently, the presence of  $\text{Ag}^+$  induces disorder at the A-site cations, resulting in the observed diffuse phase transition characteristics. Moreover, Table 1 presents the diffusion exponent  $\gamma$  for BNKT- $x$ A ceramics with  $x = 0$ –0.9% at 1 kHz, which exhibit a consistent linear relationship. Notably, the diffusion exponent  $\gamma$  exhibits a clear dependence on frequency, exhibiting higher values at higher frequencies, similar to the BNKT- $x\%$ MnCO<sub>3</sub> ceramics [43]. Our findings, in line with those of other researchers, demonstrate that the introduction of Ag leads to an increase in the diffusion exponent.

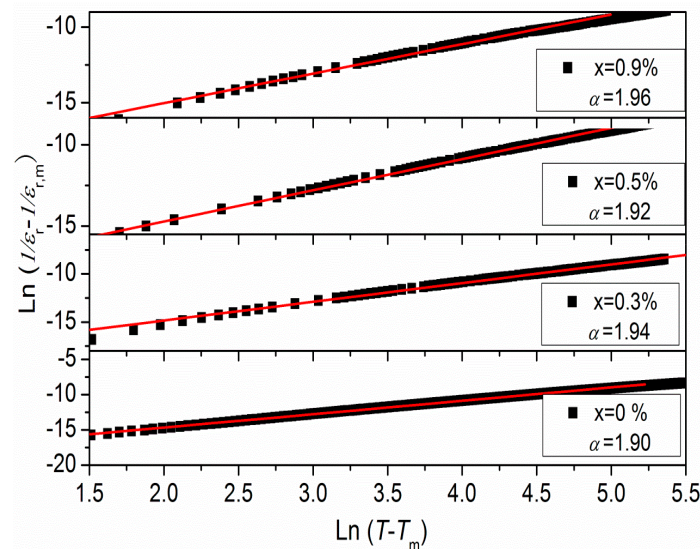


**Figure 6.**  $\ln(1/\varepsilon_r - 1/\varepsilon_{r,m})$  vs.  $\ln(T - T_m)$  for the BNKT- $x$ A piezoceramics (1 kHz).

**Table 1.** The diffusion constants and electrical properties of BNKT- $x$ A lead-free ceramics measured at 1 kHz.

$x/\%$	$\gamma$	$T_f/^\circ\text{C}$	$T_m/^\circ\text{C}$	$d_{33}/(\text{pC/N})$	$k_p$	$\varepsilon_r$	$\tan\delta$
0	1.902	114	300	115	0.218	974	0.06827
0.3	1.947	109	296	147	0.296	1199	0.06337
0.5	1.919	111	293	124	0.311	1002	0.06983
0.9	1.957	105	291	92	0.261	1104	0.0677

### 3.4. Thermal Instability

The investigation of the depolarization temperature ( $T_d$ ) in BNT-based ceramics is of utmost significance in the field of device applications. In this study,  $T_d$  was determined by analyzing the temperature-dependent characteristics of piezoelectric properties. Figure 7 illustrates the relationship between  $d_{33}$  and temperature for the ceramics. Initially,  $d_{33}$  exhibits a slight decrease as the temperature increases up to 140 °C ( $d_{33} = 45$  pC/N), followed by a significant decrease with further temperature increase. The disappearance of piezoelectric responses is observed within the temperature range of 150–160 °C. This indicates that the  $T_d$  of the piezoceramics is above 140 °C. The compound  $(\text{Li}_{0.075}\text{Na}_{0.925-x-y}\text{Ag}_y\text{K}_x)_{0.5}\text{Bi}_{0.5}\text{TiO}_3$ , discovered by D.M. Lin et al. [23], exhibits a relatively high performance ( $d_{33} = 203$  pC/N,  $k_p = 37.1\%$ ). This can be attributed to the partial substitution of Na ions in the  $\text{Na}_{0.5}\text{Bi}_{0.5}\text{TiO}_3$  lattice by  $\text{K}^+$  and  $\text{Ag}^+$ , which facilitates the rotation of ferroelectric domains and improves the electrical performance of ceramics. However, it has a low  $T_d$  of approximately 98 °C, as observed in  $(\text{Li}_{0.075}\text{Na}_{0.675}\text{Ag}_{0.075}\text{K}_{0.175})_{0.5}\text{Bi}_{0.5}\text{TiO}_3$  ceramics. Ag-doped  $\text{Bi}_{0.5}(\text{Na}_{0.825}\text{K}_{0.175})_{0.5}\text{TiO}_3$  ceramics exhibit relatively low properties compared to  $(\text{Li}_{0.075}\text{Na}_{0.675}\text{Ag}_{0.075}\text{K}_{0.175})_{0.5}\text{Bi}_{0.5}\text{TiO}_3$ , but they demonstrate a high  $T_d$  (above 140 °C, Figure 7). The elevated  $T_d$  has a crucial role in device applications. It can be ascribed to the entry of Ag ions in A-site vacancies of  $\text{Bi}_{0.5}(\text{Na}_{0.825}\text{K}_{0.175})_{0.5}\text{TiO}_3$  piezoceramics after the evaporation of partial  $\text{Na}^+$  and  $\text{K}^+$ , promoting the coupling effect between A-site cations and  $\text{TiO}_6$ , thereby increasing the depolarization temperature [19,44].

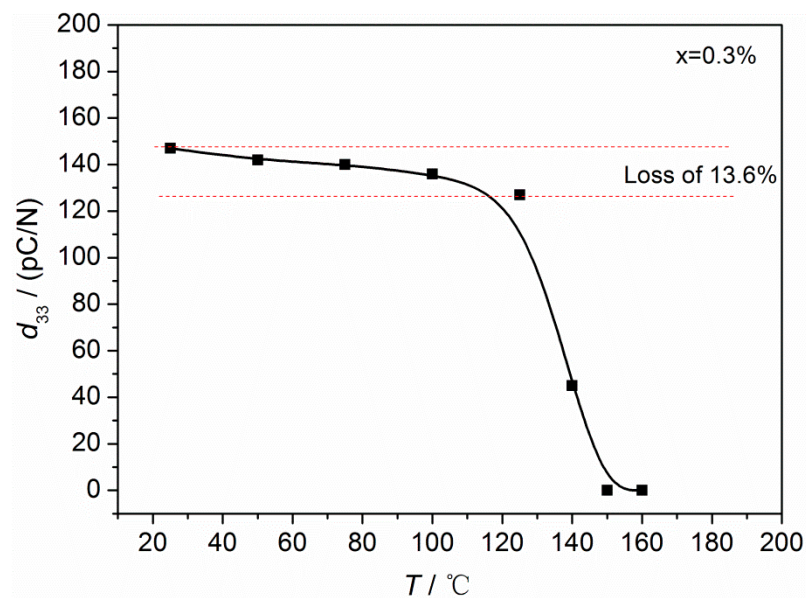


**Figure 7.** Temperature dependence of  $d_{33}$  for BNKT-xA ceramics.

In addition, within the temperature range of 25 to 125 °C, the  $d_{33}$  of BNKT-xA ceramics remains in the range of 127–147 pC/N (change in  $d_{33} \leq 13.6\%$ ). This behavior can be attributed to an underlying fact. It is suggested that the BNKT-xA piezoceramics undergo a structural transition from the R phase to the T phase within the temperature range of 25 to 125 °C, enhancing their thermal stability. However, as the temperature continues to rise, the ceramics progressively move away from the ferroelectric phase and transition towards the anti-ferroelectric phase, as depicted in Figure 5. This progressive shift ultimately results in a decrease in  $d_{33}$ .

## 4. Conclusions

The present study systematically investigates the effect of  $\text{Ag}^+$  on the crystal structure, microstructure, and electrical performance of  $(\text{K}_{0.175}\text{Na}_{0.825})_{0.5}\text{Bi}_{0.5}\text{TiO}_3$  Pb-free ceramics, which were prepared using sintering techniques. The BNKT-xA lead-free ceramics exhibit characteristic diffraction peaks associated with pure perovskites. Furthermore, the com-

positions demonstrate good sintering properties, resulting in a dense microstructure. The incorporation of Ag ions slightly affects the  $T_m$  of BNKT-xA piezoceramics by destabilizing the stability of the oxygen octahedron. The observed relaxor behavior in the ceramics is ascribed to the disorder of cations occurring at the A-sites. Simultaneously, the investigated piezoceramics have good electrical properties, characterized by a piezoelectric constant ( $d_{33}$ ) value of 147 pC/N and a coupling coefficient ( $k_p$ ) of 29.6%. The  $d_{33}$  value of the BNKT-xA piezoceramics demonstrates consistent stability within a narrow range of 127–147 pC/N (with a maximum variation of  $d_{33} \leq 13.6\%$ ) over a wide temperature range spanning from 25 to 125 °C. This finding indicates the reliable performance of the piezoceramics across various operational temperatures.

**Author Contributions:** Conceptualization, X.C.; methodology, X.C.; software, X.C.; validation, X.C.; formal analysis, X.C.; investigation, X.C.; resources, Y.L.; data curation, X.C.; writing—original draft preparation, X.C.; writing—review and editing, X.C.; visualization, X.C.; supervision, X.C.; project administration, X.C.; funding acquisition, X.C. All authors have read and agreed to the published version of the manuscript.

**Funding:** The work was funded by the Technology Fund of Guizhou Province, China (Grant No. [2020]1Y204) and the Fund of Guizhou Institute of Technology, China (Grant No. XJGC20190920; GZLGM-21).

**Institutional Review Board Statement:** Not applicable.

**Informed Consent Statement:** Not applicable.

**Data Availability Statement:** Data is available from the corresponding author upon reasonable request.

**Conflicts of Interest:** The authors declare no conflict of interest.

## References

1. Wang, K.; Shen, Z.Y.; Zhang, B.P.; Li, J.F. (K, Na)NbO<sub>3</sub>-based Lead-free Piezoceramics: Status, Prospects and Challenges. *J. Inorg. Mater.* **2014**, *29*, 13–22. [[CrossRef](#)]
2. Guo, R.; Cross, L.E.; Park, S.E.; Noheda, B.; Cox, D.E.; Shirane, G. Origin of the High Piezoelectric Response in PbZr<sub>1-x</sub>Ti<sub>x</sub>O<sub>3</sub>. *Phys. Rev. Lett.* **2000**, *84*, 5423–5426. [[CrossRef](#)] [[PubMed](#)]
3. Wodecka-Dus, B.; Goryczka, T.; Adamczyk-Habrajska, M.; Bara, M.; Dzik, J.; Szalbot, D. Dielectric and Electrical Properties of BLT Ceramics Modified by Fe Ions. *Materials* **2020**, *13*, 5623. [[PubMed](#)]
4. Craciun, E.M.; Rabaea, A.; Das, S. Cracks Interaction in a Pre-Stressed and Pre-Polarized Piezoelectric Material. *J. Mech.* **2020**, *36*, 177–182. [[CrossRef](#)]
5. Zulhadjri; Wendari, T.P.; Ikhrum, M.; Putri, Y.E.; Septiani, U.; Imelda. Enhanced dielectric and ferroelectric responses in La<sup>3+</sup>/Ti<sup>4+</sup> co-substituted SrBi<sub>2</sub>Ta<sub>2</sub>O<sub>9</sub> Aurivillius phase. *Ceram. Int.* **2022**, *48*, 10328–10332. [[CrossRef](#)]
6. Song, A.; Wang, J.; Song, J.; Zhang, J.; Li, Z.; Zhao, L. Antiferroelectricity and ferroelectricity in A-site doped silver niobate lead-free ceramics. *J. Eur. Ceram. Soc.* **2021**, *41*, 1236–1243. [[CrossRef](#)]
7. Smolenskii, G.A.; Isupov, V.A.; Agranovskaya, A.I.; Krainik, N.N. Ferroelectrics with diffuse phase transitions. *Sov. Phys. Solid State* **1961**, *2*, 2584–2594.
8. Takenaka, T. Piezoelectric properties of some lead-free ferroelectric ceramics. *Ferroelectrics* **1999**, *230*, 87–98.
9. Takenaka, T.; Nagata, H. Present status of non-lead-based piezoelectric ceramics. *Key Eng. Mater.* **1999**, *157*, 57–63.
10. Tadashi, T.; Kei-ichi, M.; Koichiro, S. (Bi<sub>1/2</sub>Na<sub>1/2</sub>)TiO<sub>3</sub>-BaTiO<sub>3</sub> System for Lead-Free Piezoelectric Ceramics. *Jpn. J. Appl. Phys.* **1991**, *30*, 2236.
11. Hong, C.-H.; Fan, Z.; Tan, X.; Kang, W.-S.; Ahn, C.W.; Shin, Y.; Jo, W. Role of sodium deficiency on the relaxor properties of Bi<sub>1/2</sub>Na<sub>1/2</sub>TiO<sub>3</sub>-BaTiO<sub>3</sub>. *J. Eur. Ceram. Soc.* **2018**, *38*, 5375–5381. [[CrossRef](#)]
12. Lin, D.; Xiao, D.; Zhu, J.; Yu, P.; Yan, H.; Li, L. Synthesis and piezoelectric properties of lead-free piezoelectric [Bi<sub>0.5</sub>(Na<sub>1-x-y</sub>K<sub>x</sub>Li<sub>y</sub>)<sub>0.5</sub>]TiO<sub>3</sub> ceramics. *Mater. Lett.* **2004**, *58*, 615–618. [[CrossRef](#)]
13. Elkechai, O.; Manier, M.; Mercurio, J.P. Na<sub>0.5</sub>Bi<sub>0.5</sub>TiO<sub>3</sub>-K<sub>0.5</sub>Bi<sub>0.5</sub>TiO<sub>3</sub> (NBT-KBT) system: A structural and electrical study. *Phys. Status Solidi A Appl. Res.* **1996**, *157*, 499–506.
14. Wang, G.; Li, Y.; Murray, C.A.; Tang, C.C.; Hall, D.A. Thermally-induced phase transformations in Na<sub>0.5</sub>Bi<sub>0.5</sub>TiO<sub>3</sub>-KNbO<sub>3</sub> ceramics. *J. Am. Ceram. Soc.* **2017**, *100*, 3293–3304. [[CrossRef](#)]
15. Xu, Q.; Xie, J.; He, Z.; Zhang, L.; Cao, M.; Huang, X.; Lanagan, M.T.; Hao, H.; Yao, Z.; Liu, H. Energy-storage properties of Bi<sub>0.5</sub>Na<sub>0.5</sub>TiO<sub>3</sub>-BaTiO<sub>3</sub>-KNbO<sub>3</sub> ceramics fabricated by wet-chemical method. *J. Eur. Ceram. Soc.* **2017**, *37*, 99–106. [[CrossRef](#)]
16. Chen, X.; Liao, Y.; Li, G. Structure and electrical properties of [(Na<sub>0.825</sub>K<sub>0.175</sub>)<sub>0.5</sub>Bi<sub>0.5</sub>]<sub>1+x</sub>TiO<sub>3</sub> piezoceramics with A-site nonstoichiometry. *J. Asian Ceram. Soc.* **2020**, *8*, 1036–1042. [[CrossRef](#)]

17. Song, G.H.; Zhang, F.Q.; Liu, F.; Liu, Z.F.; Li, Y.X. Electrical properties and temperature stability of SrTiO<sub>3</sub>-modified (Bi<sub>1/2</sub>Na<sub>1/2</sub>)TiO<sub>3</sub>-BaTiO<sub>3</sub>-(K<sub>1/2</sub>Na<sub>1/2</sub>)NbO<sub>3</sub> piezoceramics. *J. Am. Ceram. Soc.* **2021**, *104*, 4049–4057. [[CrossRef](#)]
18. Yang, H.B.; Tian, J.H.; Lin, Y.; Ma, J.Q. Realizing ultra-high energy storage density of lead-free 0.76Bi<sub>0.5</sub>Na<sub>0.5</sub>TiO<sub>3</sub>-0.24SrTiO<sub>3</sub>-Bi(Ni<sub>2/3</sub>Nb<sub>1/3</sub>)O<sub>3</sub> ceramics under low electric fields. *Chem. Eng. J.* **2021**, *418*, 129337. [[CrossRef](#)]
19. Chen, X.; Liao, Y.; Mao, L.; Deng, Y.; Wang, H.; Chen, Q.; Zhu, J.; Xiao, D.; Zhu, J.; Xu, G. Microstructure and piezoelectric properties of Li-doped Bi<sub>0.5</sub>(Na<sub>0.825</sub>K<sub>0.175</sub>)<sub>0.5</sub>TiO<sub>3</sub> piezoelectric ceramics. *Phys. Status Solidi (A)* **2009**, *206*, 1616–1619. [[CrossRef](#)]
20. Grinberg, I.; Rappe, A.M. Silver solid solution piezoelectrics. *Appl. Phys. Lett.* **2004**, *85*, 1760–1762. [[CrossRef](#)]
21. Joshi, A.; Bhatt, S.C. Investigation of dielectric properties and ferroelectric phase transition in lead-free AgNbO<sub>3</sub>. *Mater. Today Proc.* **2022**, *49*, 1607–1609. [[CrossRef](#)]
22. Wu, L.; Xiao, D.; Zhou, F.; Teng, Y.; Li, Y. Microstructure, ferroelectric, and piezoelectric properties of (1-x-y)Bi<sub>0.5</sub>Na<sub>0.5</sub>TiO<sub>3</sub>-xBaTiO<sub>3</sub>-yBi<sub>0.5</sub>Ag<sub>0.5</sub>TiO<sub>3</sub> lead-free ceramics. *J. Alloys Compd.* **2011**, *509*, 466–470. [[CrossRef](#)]
23. Lin, D.; Kwok, K.W.; Chan, H.W.L. Ferroelectric and piezoelectric properties of Bi<sub>0.5</sub>(Na<sub>0.925-x-y</sub>Li<sub>0.075</sub>K<sub>x</sub>Ag<sub>y</sub>)<sub>0.5</sub>TiO<sub>3</sub> lead-free ceramics. *J. Phys. D Appl. Phys.* **2007**, *40*, 7523. [[CrossRef](#)]
24. Liao, Y.; Xiao, D.-q.; Lin, D.; Zhu, J.; Yu, P.; Wu, L.; Wang, X.-P. Synthesis and properties of Bi<sub>0.5</sub>(Na<sub>1-x-y</sub>K<sub>x</sub>Ag<sub>y</sub>)<sub>0.5</sub>TiO<sub>3</sub> lead-free piezoelectric ceramics. *Ceram. Int.* **2007**, *33*, 1445–1448.
25. Onoe, M.; Jumonji, H. Useful Formulas for Piezoelectric Ceramic Resonators and Their Application to Measurement of Parameters. *J. Acoust. Soc. Am.* **1967**, *41*, 974–980. [[CrossRef](#)]
26. Jones, G.O.; Thomas, P.A. The tetragonal phase of Na<sub>0.5</sub>Bi<sub>0.5</sub>TiO<sub>3</sub>—A new variant of the perovskite structure. *Acta Crystallogr. Sect. B* **2000**, *56*, 426–430. [[CrossRef](#)]
27. Jones, G.O.; Thomas, P.A. Investigation of the structure and phase transitions in the novel A-site substituted distorted perovskite compound Na<sub>0.5</sub>Bi<sub>0.5</sub>TiO<sub>3</sub>. *Acta Crystallogr. Sect. B* **2002**, *58*, 168–178. [[CrossRef](#)]
28. Lei, N.; Zhu, M.; Yang, P.; Wang, L.; Wang, L.; Hou, Y.; Yan, H. Effect of lattice occupation behavior of Li<sup>+</sup> cations on microstructure and electrical properties of (Bi<sub>1/2</sub>Na<sub>1/2</sub>)TiO<sub>3</sub>-based lead-free piezoceramics. *J. Appl. Phys.* **2011**, *109*, 054102. [[CrossRef](#)]
29. Shannon, R. Revised effective ionic radii and systematic studies of interatomic distances in halides and chalcogenides. *Acta Crystallogr. Sect. A Cryst. Phys. Diffr. Theor. Gen. Crystallogr.* **1976**, *32*, 751–767. [[CrossRef](#)]
30. Akram, F.; Ahmed Malik, R.; Hussain, A.; Song, T.-K.; Kim, W.-J.; Kim, M.-H. Temperature stable dielectric properties of lead-free BiFeO<sub>3</sub>-BaTiO<sub>3</sub> modified with LiTaO<sub>3</sub> ceramics. *Mater. Lett.* **2018**, *217*, 16–19. [[CrossRef](#)]
31. Wang, B.; Luo, L.; Ni, F.; Du, P.; Li, W.; Chen, H. Piezoelectric and ferroelectric properties of (Bi<sub>1-x</sub>Na<sub>0.8</sub>K<sub>0.2</sub>La<sub>x</sub>)<sub>0.5</sub>TiO<sub>3</sub> lead-free ceramics. *J. Alloys Compd.* **2012**, *526*, 79–84. [[CrossRef](#)]
32. Jones, G.O.; Kreisel, J.; Thomas, P.A. A structural study of the (Na<sub>1-x</sub>K<sub>x</sub>)<sub>0.5</sub>Bi<sub>0.5</sub>TiO<sub>3</sub> perovskite series as a function of substitution (x) and temperature. *Powder Diffr.* **2012**, *17*, 301–319. [[CrossRef](#)]
33. Chen, X.; Ai, C.; Yang, Z.; Ni, Y.; Yin, X.; You, J.; Li, G. Mitigation of Thermal Instability for Electrical Properties in CaZrO<sub>3</sub>-Modified (Na, K, Li) NbO<sub>3</sub> Lead-Free Piezoceramics. *Materials* **2023**, *16*, 3720. [[CrossRef](#)] [[PubMed](#)]
34. Sasaki, A.; Chiba, T.; Mamiya, Y.; Otsuki, E. Dielectric and Piezoelectric Properties of (Bi<sub>0.5</sub>Na<sub>0.5</sub>)TiO<sub>3</sub>-(Bi<sub>0.5</sub>K<sub>0.5</sub>)TiO<sub>3</sub> Systems. *Jpn. J. Appl. Phys.* **1999**, *38*, 5564. [[CrossRef](#)]
35. Kazushige, Y.; Yuji, H.; Hajime, N.; Tadashi, T. Electrical Properties and Depolarization Temperature of (Bi<sub>1/2</sub>Na<sub>1/2</sub>)TiO<sub>3</sub>-(Bi<sub>1/2</sub>K<sub>1/2</sub>)TiO<sub>3</sub> Lead-free Piezoelectric Ceramics. *Jpn. J. Appl. Phys.* **2006**, *45*, 4493.
36. Li, Y.; Chen, W.; Zhou, J.; Xu, Q.; Sun, H.; Xu, R. Dielectric and piezoelectric properties of lead-free (Na<sub>0.5</sub>Bi<sub>0.5</sub>)TiO<sub>3</sub>-NaNbO<sub>3</sub> ceramics. *Mater. Sci. Eng. B* **2004**, *112*, 5–9. [[CrossRef](#)]
37. Sakata, K.; Takenaka, T.; Naitou, Y. Phase-Relations, Dielectric And Piezoelectric Properties Of Ceramics In the System (Bi<sub>0.5</sub>Na<sub>0.5</sub>)TiO<sub>3</sub>-PbTiO<sub>3</sub>. *Ferroelectrics* **1992**, *131*, 219–226. [[CrossRef](#)]
38. Hou, Y.; Zhu, M.; Gao, F.; Wang, H.; Wang, B.; Yan, H.; Tian, C. Effect of MnO<sub>2</sub> Addition on the Structure and Electrical Properties of Pb(Zn<sub>1/3</sub>Nb<sub>2/3</sub>)<sub>0.20</sub>(Zr<sub>0.50</sub>Ti<sub>0.50</sub>)<sub>0.80</sub>O<sub>3</sub> Ceramics. *J. Am. Ceram. Soc.* **2004**, *87*, 847–850. [[CrossRef](#)]
39. Hou, Y.D.; Chang, L.M.; Zhu, M.K.; Song, X.M.; Yan, H. Effect of Li<sub>2</sub>CO<sub>3</sub> addition on the dielectric and piezoelectric responses in the low-temperature sintered 0.5PZN–0.5PZT systems. *J. Appl. Phys.* **2007**, *102*, 084507. [[CrossRef](#)]
40. Lide, D.R.E. *Handbook of Chemistry and Physics*, 90th ed.; CRC Press: Boca Raton, FL, USA, 2009.
41. Zhu, M.K.; Lu, P.X.; Hou, Y.D.; Wang, H.; Yan, H. Effects of Fe<sub>2</sub>O<sub>3</sub> addition on microstructure and piezoelectric properties of 0.2 PZN-0.8 PZT ceramics. *J. Mater. Res.* **2005**, *20*, 2670–2675.
42. Uchino, K.; Nomura, S. Critical exponents of the dielectric constants in diffused-phase-transition crystals. *Ferroelectrics* **1982**, *44*, 55–61. [[CrossRef](#)]
43. Jiang, X.P.; Li, L.Z.; Zeng, M.; Chan, H.L.W. Dielectric properties of Mn-doped (Na<sub>0.8</sub>K<sub>0.2</sub>)<sub>0.5</sub>Bi<sub>0.5</sub>TiO<sub>3</sub> ceramics. *Mater. Lett.* **2006**, *60*, 1786–1790. [[CrossRef](#)]
44. Thomas, N.W. A new framework for understanding relaxor ferroelectrics. *J. Phys. Chem. Solids* **1990**, *51*, 1419–1431. [[CrossRef](#)]

**Disclaimer/Publisher’s Note:** The statements, opinions and data contained in all publications are solely those of the individual author(s) and contributor(s) and not of MDPI and/or the editor(s). MDPI and/or the editor(s) disclaim responsibility for any injury to people or property resulting from any ideas, methods, instructions or products referred to in the content.